

Membership and Segregation Effects in the Young Open Cluster NGC 6530 *

Jun-Liang Zhao¹, Li Chen¹ and Wen Wen^{1,2}

¹ Shanghai Astronomical Observatory, Chinese Academy of Sciences, Shanghai 200030;
chenli@shao.ac.cn

² Shanghai University, Shanghai 200444

Received 2005 November 16; accepted 2006 February 20

Abstract From photographic plate data of Shanghai Astronomical Observatory with a time baseline of 87 years, proper motions and membership probabilities of 364 stars in the open cluster NGC 6530 region are reduced. On the basis of membership determination, luminosity function and segregation effect of the cluster are discussed with details. Spatial mass segregation is obviously present in NGC 6530 while there is no clear evidence for a velocity-mass (or velocity-luminosity) dependence. The observed spatial mass segregation for NGC 6530 might be due to a combination of initial conditions and relaxation process.

Key words: open clusters and associations: individual (NGC 6530)

1 INTRODUCTION

Young open clusters are important stellar systems for understanding star formation processes. In a very young cluster, most of the low-mass stars are still in their pre-main-sequence (PMS) stage and one can derive Initial Mass Function (IMF) which are still little affected by stellar and dynamical evolution (Herbst & Miller 1982; Sung et al. 1997, 1998). NGC 6530 is an example of an extremely young open cluster and has been the subject of a number of previous studies. The cluster is located in the eastern part of the Lagoon nebula (M8), which is one of the brightest nebulae and HII regions closest to us (Rauw et al. 2002). Its center is in a direction not far from that of the Galactic center. Its equatorial coordinates are $(\alpha, \delta)_{2000} = (18^{\text{h}}04^{\text{m}}.6, -24^{\circ}20')$ and its galactic coordinates are $(l^{\text{II}}, b^{\text{II}} = 6.13^{\circ}, -1.38^{\circ})$. In 1957, Walker (1957) investigated the photoelectric magnitudes and colors of 118 stars in the NGC 6530 region and proposed that a band of its low mass members lying above the main sequence is made up of pre-main sequence stars (PMS) that are still at the gravitational contraction stage. Subsequently, the properties of this very young cluster have been extensively studied by different authors, with its age estimated as 1.5–2.0 million years (van Altena & Jones 1972; Sagar & Joshi 1978; Sung et al. 2000), and its distance from the Sun estimated in the range 0.6–2.0 kpc (Walker 1957; The 1960; Walker 1961; Hiltner et al. 1965; Altena & Jones 1972; Kilambi 1977; Sagar & Joshi 1978; Chini & Neckel 1981; Loktin et al. 1997; Sung et al. 2000; Loktin & Beshenov 2001; Prisinzano et al. 2005).

It should be noted that a reasonable membership determination of stars is crucial for studies on a star cluster. In 1972, for the first time van Altena & Jones (1972, hereafter AJ) determined the membership probabilities of 363 stars in a $60' \times 32'$ region centered on NGC 6530 from relative proper motion data with a time baseline of 34 years, and they found 76 member stars with probabilities higher than 0.5.

* Supported by the National Natural Science Foundation of China.

In this paper, we use photographic plate material with longer time baselines to determine the proper motions (in Section 2) and membership (in Section 3) of stars in the region of NGC 6530, and make further studies on the cluster based on our membership determinations, such as the color-magnitude diagram (Section 4) and the luminosity function and mass segregation effects (Section 5). A summary is given in Section 6.

2 PLATE MATERIAL AND PROPER MOTION REDUCTION

2.1 Plate Material and Measurements

The six photographic plates used for proper motion reduction of the open cluster NGC 6530 were all taken by the 40 cm double astrograph with focal length of 6.9 m at Sheshan (Zô–Sè) Station of Shanghai Astronomical Observatory, Chinese Academy of Sciences, with two first epoch plates and four second epoch ones taken in 1912 and 1999 respectively, with a time baseline extending over 87 years. The field of view is $2^\circ \times 2.5^\circ$ and $1.5^\circ \times 1.5^\circ$ for the first and the second epoch plates, respectively. The plates were taken with no filters and their emulsion sensitive range was close to the B-passband. The observation parameters are listed in Table 1.

Table 1 Plate Parameters of NGC 6530

Plate No.	Date	Exposure time (min)	Number of Star
CL 371	1912–08–04	–	586
CL 372	1912–08–04	–	603
CL 99008	1999–05–19	30	354
CL 99009	1999–05–19	30	314
CL 99010	1999–08–05	30	667
CL 99011	1999–08–05	30	501

All the Sheshan plates were measured using the PDS- instrument of Dominion Astrophysical Observatory (DAO) in Canada. For each plate, a full-area scanning was performed over a $60' \times 60'$ cluster central region. Both the scan step and line feed were 20 micron, the size of a scanning pixel was 20.5×20.5 micron and the R scanning mode and scanning speed of 15 mm s^{-1} were used. From the full-area scanning data, stellar images were extracted and their rectangular coordinates x and y were obtained with the DAOFIND and PDSRED programs provided by the DAO. In order to cross-identifying the stellar images, their measured x and y coordinates were transformed to the same coordinate system by a linear transformation using six plate constants. Stars with residual errors greater than $15 \mu\text{m}$ were excluded. Every single one of these stars appears on at least one plate of each epoch.

2.2 Proper Motion Reduction

From the cross identification 365 stars were obtained, including 79 stars listed in the Tycho-2 Catalogue; these are selected as the reference stars for proper motion reduction. For these 79 stars the positions and proper motions from the Tycho-2 Catalogue were adopted.

The central overlapping technique (Russell 1967; Wang et al. 1996) was used for reduction of the stellar constants including proper motions of 365 stars. In the reduction six linear and six quadratic terms were used and the catalogue positions and proper motions of the 79 Tycho-2 stars, weighted by their errors, were included as observations. During the iterative solution only one star with an extraordinarily large residual error was deleted, thus we finally have the positions and proper motions of 364 stars in the NGC 6530 region, which can be used to derive the distribution parameter and membership estimation of the cluster.

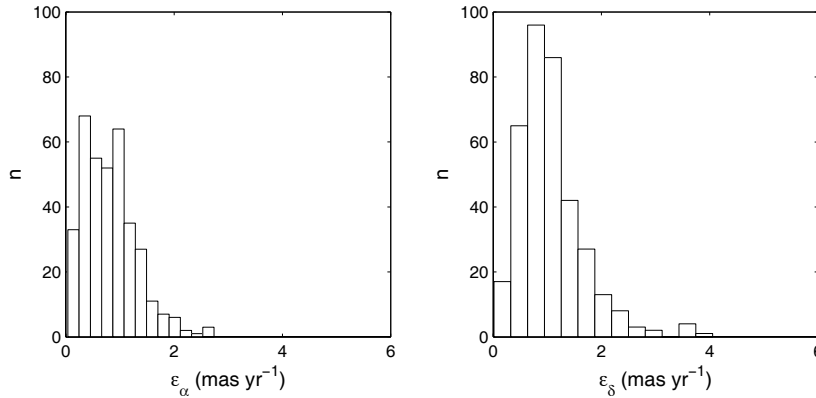
The estimates of observational accuracies of both positions and proper motions for the 364 stars are listed in Table 2. The average single coordinate proper motion error for all 364 stars is $\pm 1.09 \text{ mas yr}^{-1}$, while the average error for stars that appeared on all six plates is 0.94 mas yr^{-1} . Table 3 shows the dependence of the errors of proper motions on the number of plates, and Figure 1 gives the histogram of the frequency distribution of the errors in proper motion of the 364 stars.

Table 2 Errors of Positions and Proper Motions of 364 Stars

Parameter	Mean error	Maximum error
α	$\pm 0.003^s$	$\pm 0.014^s$
δ	$\pm 0.06''$	$\pm 0.16''$
$\mu_{\alpha \cos \delta}$	$\pm 0.95 \text{ mas yr}^{-1}$	$\pm 2.74 \text{ mas yr}^{-1}$
μ_{δ}	$\pm 1.21 \text{ mas yr}^{-1}$	$\pm 4.05 \text{ mas yr}^{-1}$

Table 3 Mean Errors of Proper Motions of Stars vs. Number of Plates

Number of plates	Number of star	ε_x	ε_y	ε
		mas yr ⁻¹	mas yr ⁻¹	mas yr ⁻¹
6	125	0.89	0.98	0.94
5	70	1.03	1.35	1.20
4	103	0.86	1.17	1.03
3	53	1.02	1.47	1.26
2	13	1.45	1.60	1.53
total	364	0.95	1.21	1.09

**Fig. 1** Histograms of the frequency distribution of the proper motion errors.

3 MEMBERSHIP DETERMINATION

For membership determination of star clusters from data of relative proper motion, the basic mathematical model that Vasilevskis et al. (1958) suggested was widely used and the approach based upon the maximum likelihood principle that Sanders (1971) developed has been adopted to find the distribution parameters of the clusters and the membership probabilities of individual stars in the cluster region. Because of the importance of correctly identifying member stars of clusters, much improvement in the method of determining proper motion membership have been implemented (Cabrera-Cano & Alfaro 1985; Jones & Walker 1988; Girard et al. 1989; Zhao & He 1990; Balaguer-Núñez et al. 1998).

3.1 Mathematical Model

In addition to Vasilevskis et al.'s model (Vasilevskis et al. 1958), the following factors are also taken into account in this paper for the membership determination of NGC 6530: (i) Different observational accuracies in the proper motion of different stars; (ii) In the position space, the surface number density of cluster members is a function of the radius from the cluster center and follows approximately a Gaussian profile, while the distribution of field stars should be uniform over the field. Then, the distribution function of proper

motions in a cluster region can be written as

$$\Phi = \Phi_f + \Phi_c, \quad (1)$$

where Φ_f and Φ_c are the distributions for field stars and cluster members, respectively:

$$\begin{aligned} \Phi_f = & \Psi_f(r_i) \cdot \frac{1}{2\pi(1-\rho^2)^{1/2}(\sigma_{x0}^2 + \varepsilon_{xi}^2)^{1/2}(\sigma_{y0}^2 + \varepsilon_{yi}^2)^{1/2}} \\ & \cdot \exp \left\{ -\frac{1}{2(1-\rho^2)} \left[\frac{(\mu_{xi} - \mu_{xf})^2}{\sigma_{x0}^2 + \varepsilon_{xi}^2} \right. \right. \\ & \left. \left. - \frac{2\rho(\mu_{xi} - \mu_{xf})(\mu_{xi} - \mu_{xf})}{(\sigma_{x0}^2 + \varepsilon_{xi}^2)^{1/2}(\sigma_{y0}^2 + \varepsilon_{yi}^2)^{1/2}} + \frac{(\mu_{yi} - \mu_{yf})^2}{\sigma_{y0}^2 + \varepsilon_{yi}^2} \right] \right\}, \end{aligned} \quad (2)$$

$$\begin{aligned} \Phi_c = & \Psi_c(r_i) \cdot \frac{1}{2\pi(\sigma_0^2 + \varepsilon_{xi}^2)^{1/2}(\sigma_0^2 + \varepsilon_{yi}^2)^{1/2}} \\ & \cdot \exp \left\{ -\frac{1}{2} \left[\frac{(\mu_{xi} - \mu_{xc})^2}{\sigma_0^2 + \varepsilon_{xi}^2} + \frac{(\mu_{yi} - \mu_{yc})^2}{\sigma_0^2 + \varepsilon_{yi}^2} \right] \right\}, \end{aligned} \quad (3)$$

where (μ_{xi}, μ_{yi}) is the proper motion of the i -th star and $(\varepsilon_{xi}, \varepsilon_{yi})$ the corresponding observational error, both of which can be obtained from the proper motion reduction, (μ_{xf}, μ_{yf}) and (μ_{xc}, μ_{yc}) are the centers of the field stars and cluster members in the vector-point-diagram (VDP), respectively; $(\sigma_{x0}, \sigma_{y0})$ and σ_0 the respective intrinsic proper motion dispersions; ρ the correlation coefficient of the proper motion distribution of the field stars.

By assuming a homogeneous distribution ψ_f with the average number density n_f for field stars and a Gaussian distribution ψ_c with the central density n_0 for the cluster stars, we have

$$\psi_f = n_f \quad \text{and} \quad \psi_c(r_i) = n_0 \exp\left(-\frac{r_i^2}{2\sigma_\alpha^2}\right),$$

with α and r_i the dispersion of the positional distribution of member stars and the radial distance of the i th stars from the cluster center. Write $g = n_0/n_f$ and let Ψ_f and Ψ_c be the normalized ψ_f and ψ_c , that is $\Psi_f + \Psi_c = 1$, then we have

$$\begin{aligned} \Psi_f(r_i) &= \frac{1}{1 + g \exp^{-1}\left(-\frac{r_i^2}{2\sigma_\alpha^2}\right)}, \\ \Psi_c(r_i) &= \frac{1}{1 + g^{-1} \exp^{-1}\left(-\frac{r_i^2}{2\sigma_\alpha^2}\right)}. \end{aligned} \quad (4)$$

Then, we have, for the likelihood function for the $N (= 364)$ stars,

$$L(\theta_j; j = 1, \dots, 10) = \ln \prod_{i=1}^N \Phi(\mu_{xi}, \mu_{yi}) = \sum_{i=1}^N \ln \Phi(\mu_{xi}, \mu_{yi}), \quad (5)$$

where $\theta_j (j = 1, \dots, 10) \equiv (\mu_{xf}, \mu_{yf}, \mu_{xc}, \mu_{yc}, \sigma_{x0}, \sigma_{y0}, \sigma_0, \rho, g, \sigma_\alpha)$ are the 10 distribution parameters to be determined.

The values of these parameters were estimated by the maximum likelihood method, the uncertainty of the parameter estimation was evaluated by the second derivatives of the likelihood function (Zhao et al. 1987). Then the membership probability of the i -th star can be calculated:

$$p_i = \frac{\Phi_c}{\Phi} = \frac{\Phi_c}{\Phi_f + \Phi_c}. \quad (6)$$

3.2 Distribution Parameters

Table 4 gives the maximum likelihood estimates of the distribution parameters and the corresponding uncertainties. It can be seen from the results that the 10 distribution parameters are all determined with satisfactorily high accuracies and the intrinsic proper motion dispersion σ_0 (2.41 mas yr^{-1}) of the cluster members is obviously and satisfactorily less than the σ_{x0}/σ_{y0} ($9.19/8.71 \text{ mas yr}^{-1}$) of the field stars.

Table 4 Estimates of Distribution Parameters

Parameter	Estimate and uncertainty (mas yr^{-1})
μ_{xc}	2.59 ± 0.16
μ_{yc}	-3.48 ± 0.17
μ_{xf}	3.62 ± 0.34
μ_{yf}	-7.69 ± 0.88
σ_0	2.41 ± 0.40
σ_{x0}	9.19 ± 0.17
σ_{y0}	8.71 ± 0.36
ρ	0.22 ± 0.07
σ_α	24.45 ± 0.70
g	8.84 ± 0.21

3.3 Membership Probabilities

With the distribution parameters listed in Table 4, we can calculate the membership probabilities of individual stars in the cluster region from Equation (6). Figure 2 is the histogram of membership probabilities of 364 stars in the region. It can be seen that our membership determination is quite effective, and there are only a few stars with probability values around 0.5; specifically, there are only 16 stars (or 4.4% of the total number of 364) with $0.3 \leq p \leq 0.7$. On the other hand, there are many stars with high probabilities; 250 stars with $p \geq 0.9$ and 201 with $p \geq 0.95$, values so high that these stars can be reasonably used as a sample of cluster members in further studies. Table 5 gives the first five lines of our astrometric and membership probability file for the 364 stars in the NGC 6530 region: the successive columns give the serial number of the star, its right ascension and declination relative to J2000.0 equator and equinox, at epoch J2000.0; its absolute proper motion in right ascension and declination and the corresponding standard errors (in units of mas yr^{-1}); and lastly, its membership probability. The whole table is available on-line in a machine-readable form.

Table 5 Proper Motions and Membership Probabilities of 364 Stars in the Region of NGC 6530^a

No.	R.A.(J2000.0)	DEC(J2000.0)	$\mu_\alpha \cos \delta$ [mas yr^{-1}]	σ_{PA} [mas yr^{-1}]	μ_δ [mas yr^{-1}]	σ_{PD} [mas yr^{-1}]	prb
1	18 02 04.536	-24 38 05.35	3.70	1.06	-8.79	0.60	0.66
2	18 02 05.851	-24 09 18.21	3.35	0.63	-6.56	0.80	0.92
3	18 02 06.131	-24 45 22.28	2.46	0.51	2.80	0.39	0.58
4	18 02 06.399	-24 48 46.35	0.45	1.41	0.92	1.82	0.81
5	18 02 07.839	-24 15 22.06	-1.47	0.63	-1.92	1.41	0.90
...

^a : This table is available only on-line as a machine-readable table. A portion is shown here for guidance regarding for its form and content.

3.4 Surface Number Density Profiles of Cluster Members and Field Stars

To evaluate the above results on membership determination, we examined the surface number density profiles for cluster members and field stars. Figure 3 shows respectively the 2-D positional distributions of field stars with $p \leq 0.1$ (left) and cluster members with $p \geq 0.9$ (right).

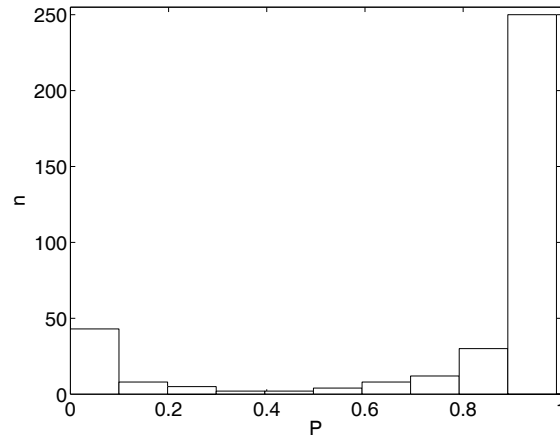


Fig. 2 Histograms of membership probabilities of 364 stars in the region of open cluster NGC 6530.

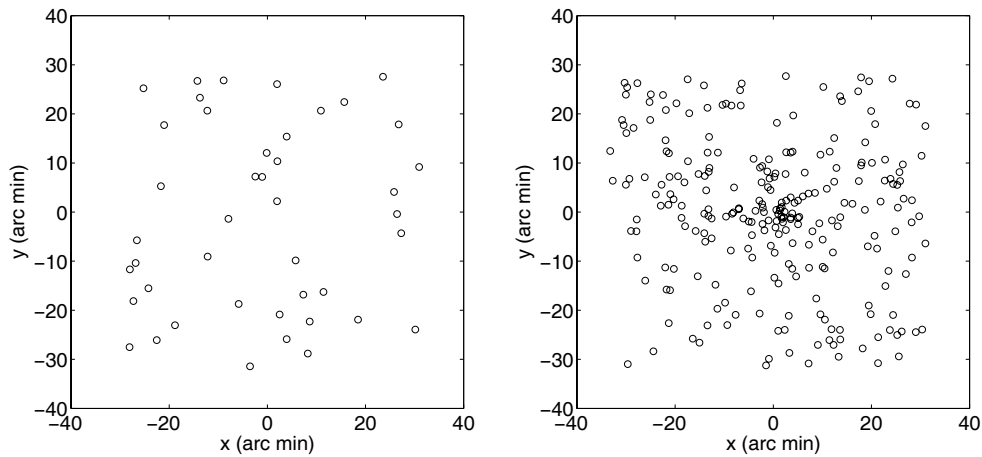


Fig. 3 Positional distribution of stars in the NGC 6530 region. left: field star with $p \leq 0.1$; right: cluster members with $p \geq 0.9$

The cluster members exhibit an obvious concentration on the sky, while this is not the case for the field stars. Figure 4 displays the radial surface number density profiles of cluster members ($p \geq 0.9$) and field stars ($p \leq 0.1$). The two profiles are completely different, with the field profile quite flat and the cluster profile exhibiting a normal distribution, easily confirmed by a statistical test. This result shows once again that our results on membership determination are reasonable and reliable.

3.5 Comparison with the Member Sample of AJ

Our Sheshan plates covered about twice the area as in AJ, and include almost the whole of the latter. On the other hand, the AJ sample is around one magnitude fainter than ours. So the two samples have nearly the same number of stars. Cross-identification yielded 200 stars in common. Hereafter we will write p for the membership probability determined by us and p' for that of AJ. Among the stars in common, 70 stars have $p' \geq 0.5$ (note $p' \geq 0.5$ is the criterion adopted by AJ for cluster member in their sample), most of which (67 out of 70) have $p \geq 0.9$. On the other hand, among the other 130 stars with $p' < 0.5$, 91 have $p \geq 0.9$,

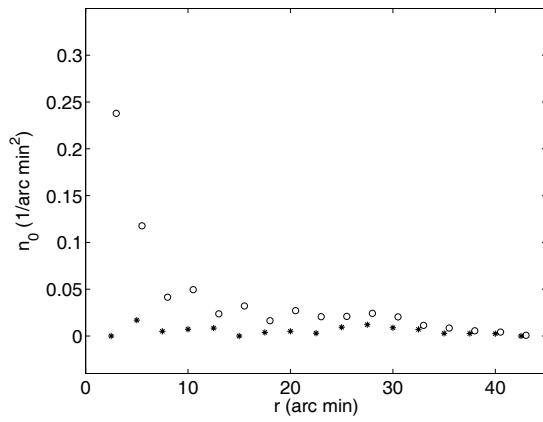


Fig. 4 Radial number density profiles of stars in the NGC 6530 region. *: field stars; o: cluster members.

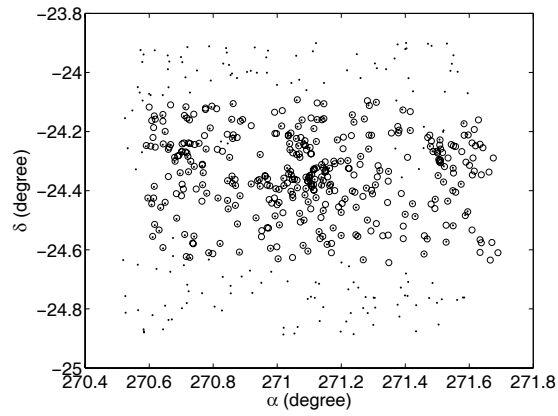


Fig. 5 Cross-identification between the stellar images in the AJ sample (open circles) and our sample (dots).

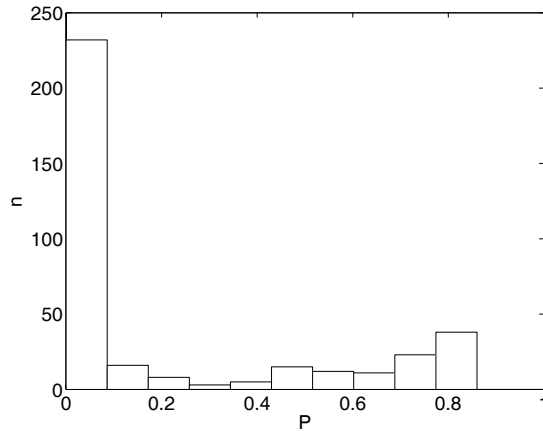


Fig. 6 Histogram of membership probabilities of 363 stars in the AJ sample.

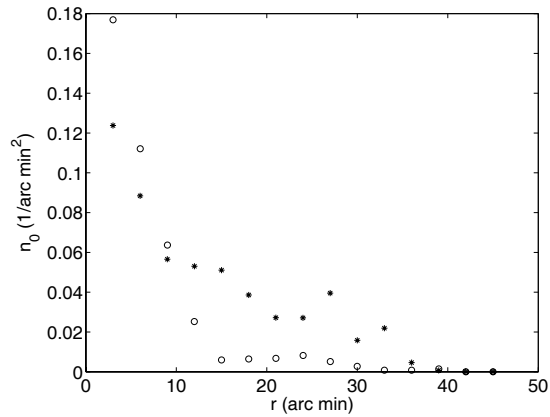


Fig. 7 Surface number density profiles of stars in the NGC 6530 region in the AJ sample. *: field stars with $p' \leq 0.1$; o: member stars with $p' \geq 0.5$.

which shows that, judged by our result, quite a large portion of the AJ sample have their membership probabilities underestimated. Figure 5 shows the cross-identification between the stellar images in the AJ and our observational samples.

For a given cluster, the effectiveness of membership determination is dependent on the accuracy of the proper motions and on the mathematical model adopted. For NGC 6530, the proper motion accuracies are much the same for the AJ and our samples. On the other hand, the mathematical model used by AJ did not take into account the factors that observed errors of stellar proper motions might differ from star to star and that the surface number density distribution of cluster members should not be uniform. Figure 6 shows the histogram of p' s in the AJ sample, where one can see that the distinction between cluster members and field stars is not clear and that there are few stars with higher probabilities (no stars have $p' \geq 0.9$). Figure 7 shows the radial number density profiles of cluster members and field stars in the AJ sample, 88 stars with probabilities $p' \geq 0.5$ having been adopted as cluster members and 240 stars with $p' \leq 0.1$ as field ones.

Here both profiles exhibit a significant concentration, which is inconsistent with the expectation that the field stars should not do so.

From the preceding discussion we conclude that our sample of cluster members, obtained from independent photographic observations and based on an improved mathematic model for proper motion membership, covers a larger observed area and contains more cluster stars, and so is more reliable for future studies of the open cluster NGC 6530.

4 THE COLOR-MAGNITUDE DIAGRAM

To obtain the B and V magnitudes of the stars in our sample, the instrumental magnitudes B_p by the PDS at DAO are compared with the B magnitudes of AJ for the stars in common. The result is shown in Figure 8. There is, except for a few stars, an obvious close correlation between the two, which we use to convert our B_p magnitudes to the B magnitudes in the UBV system. Moreover, we take the V magnitudes of individual stars from the AJ catalogue when constructing the CMD.

Figure 9 shows the color-magnitude diagram (CMD) of all the 137 stars with $p \geq 0.95$ that have V and B magnitudes available. The main sequence (MS) of this young cluster is quite wide, and this could be due to different causes, e.g., variable reddening across the observed area (which we expected as the main cause), photometric (and calibration) errors and the possible presence of a number of binary stars. Besides, and interestingly, there are quite a few stars in the red part of the CMD at $B=11.0-12.3$, $(B-V)=1.1-1.7$, forming an obvious red clump. On the other hand, the effect of contamination by field stars should not be significant. Actually, since the stars used in the CMD all have membership probabilities higher than 0.95, by the formula $N_f = 137 - \sum p_i$, where p_i is the membership probability of individual star on the CMD, we can estimate that the number of field stars appearing on the diagram is only $N_f \approx 3$.

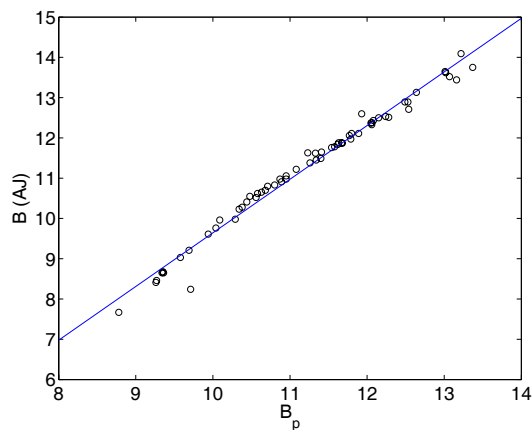


Fig. 8 Comparison between the instrumental magnitudes B_p and the AJ B magnitudes for the stars in common.

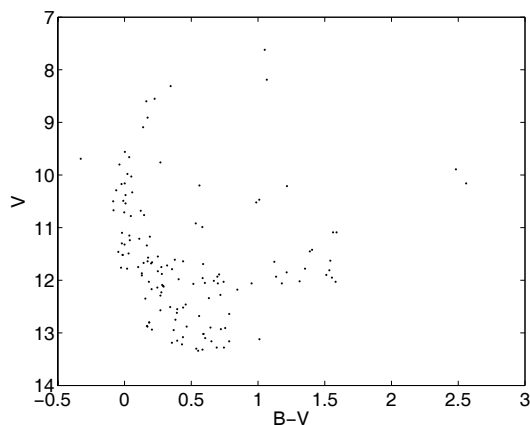


Fig. 9 CMD of the stars with membership probabilities higher than 0.95 in NGC 6530.

Another feature of the CMD is its well-defined blue envelope, to the left side of which no stars are present. This observational fact is very likely due to the presence of the giant molecular cloud, which prevents us from seeing field stars beyond, most of which should be main sequence stars. The blue envelope has been confirmed by Prisinzano et al. (2005) for a much fainter magnitude range, even though there were no individual membership probabilities available in their sample. On the other hand, since the cluster is very young, some of the stars to the right side of the main sequence may be pre-main sequence stars that had not enough evolution time to reach the main sequence of the cluster, as pointed out by some authors (e.g. Prisinzano et al. 2005).

5 LUMINOSITY FUNCTION AND SEGREGATION EFFECTS

5.1 Luminosity Function and the Mass Segregation

Figure 10 shows the M_B luminosity function of 250 stars with membership probabilities higher than 0.9 in the NGC 6530 region in our sample with an adopted distance of the cluster of $r = 1250$ pc (Prisinzano et al. 2005) and a reddening of $E_{B-V} = 0.35$ (Sung et al. 2000), leading to a distance module of $(m - M)_B = 11.57$.

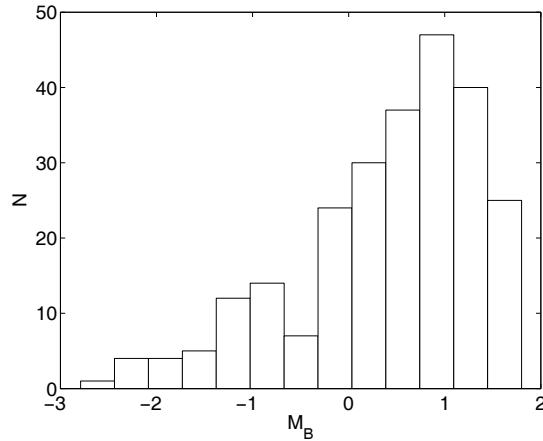


Fig. 10 Luminosity function of 250 stars in the NGC 6530 region with membership probabilities higher than 0.9.

Some authors have documented that the radial distributions of high and low mass member stars in many open clusters differ significantly (van den Bergh & Sher 1960; Larson 1982; Zhao et al. 1996), which means the presence of mass segregation in these clusters. To discuss the segregation effect in NGC 6530, we first examined the luminosity functions of member stars in different parts of the cluster. Figures 11a (left) and 11b (right) show the luminosity functions of cluster members in the inner (radial distance $d \leq 20'$) and outer ($d > 20'$) parts of the cluster. Here, mass segregation is readily seen: the fraction of brighter stars (or more massive stars) is higher in the inner than in the outer part.

To further examine the segregation effect in NGC 6530, we investigate the radial density distributions of member stars ($p \geq 0.9$) of different masses in the cluster. See Figure 12. Here, mass segregation manifest: while the low-mass (fainter) stars are spread throughout the cluster, including the core, the high-mass (brighter) stars are predominantly located in the inner regions.

We also calculated the half-light radii for three magnitude ranges in the cluster, and the results are listed in Table 6. It can be seen that the brighter members have, on average, smaller half-light radii: another indication of the existence of mass segregation in NGC 6530.

Table 6 Half-light Radii of Cluster Members with Various B Magnitudes and $p \geq 0.9$

B	Star number	Half-light radius
All the stars	250	21.5'
$B < 12.0$	87	12.9'
$12.0 \leq B < 13.0$	80	21.0'
$B \geq 13.0$	83	24.7'

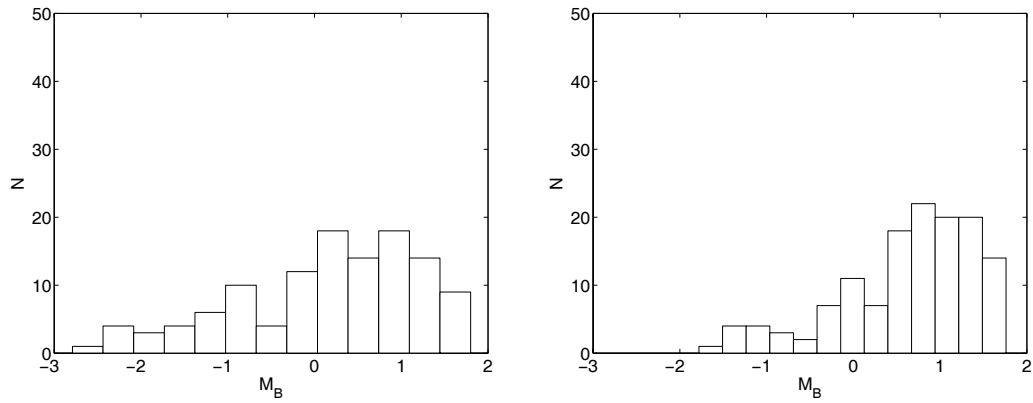


Fig. 11 Left: Luminosity function the 117 member stars in the inner area ($d \leq 20'$); right: that of the 133 member stars in the outer area ($d > 20'$).

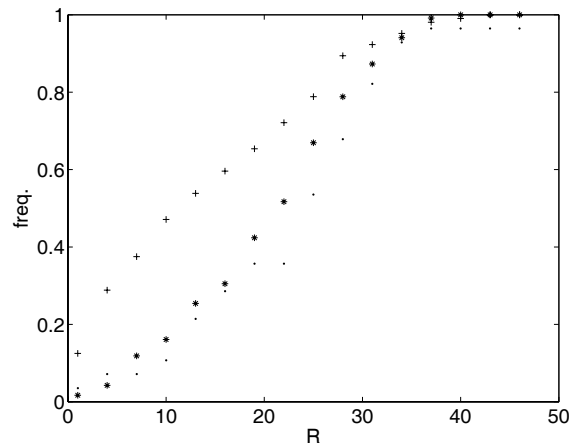


Fig. 12 Normalized cumulative radial number density profiles for NGC 6530 members with $m_B < 12.0$ (+), $12.0 \leq m_B < 13.0$ (*), and $m_B \geq 13.0$ (•). R is in units of arcmin.

5.2 Velocity-mass Relation

If there is indeed segregation in NGC 6530 and if it solely results from two-body relaxation and energy equipartition, then one should find some evidence not only in the spatial distribution, but also in the velocity distribution: the more massive members will have a smaller velocity dispersion than the less massive ones have.

Accordingly, for members of different magnitude ranges, the intrinsic dispersions σ_{int} and the corresponding uncertainties from the observed dispersions σ_{obs} and the mean errors of the stellar proper motions were investigated. The final results are given in Table 7, where the successive columns are: membership probability, B magnitude range, sub-sample size, x and y proper motion dispersions, and the weighted proper motion dispersion. It can be seen that the intrinsic proper motion dispersions are not significantly different for the various magnitude groups, especially for the member stars with higher membership probabilities ($p \geq 0.95$). Thus there is no definitive evidence that points to a velocity-mass correlation in NGC 6530.

Table 7 Velocity-luminosity Dependence of Members in NGC 6530

p	B	n	$\langle\sigma_x^2\rangle^{1/2}$	$\langle\sigma_y^2\rangle^{1/2}$	$\langle\sigma\rangle$
≥ 0.90	< 11	41	1.67 ± 0.22	1.22 ± 0.25	1.46 ± 0.24
	11 – 12	46	1.65 ± 0.22	1.71 ± 0.26	1.68 ± 0.24
	12 – 13	80	2.09 ± 0.21	1.59 ± 0.21	1.86 ± 0.21
	≥ 13	83	1.65 ± 0.18	2.09 ± 0.23	1.89 ± 0.21
≥ 0.95	< 11	35	1.07 ± 0.19	1.18 ± 0.26	1.13 ± 0.23
	11 – 12	40	1.32 ± 0.21	1.60 ± 0.27	1.47 ± 0.24
	12 – 13	63	1.57 ± 0.19	1.32 ± 0.23	1.45 ± 0.21
	≥ 13	63	1.26 ± 0.20	1.59 ± 0.23	1.44 ± 0.22

The traditional explanation for mass segregation in space in an open star cluster is that it results from energy equipartition or from approach to equipartition. However, it seems to us that this is not the case for NGC 6530, which is a very young cluster with an age of only around 2 Myr. As pointed out by McNamara & Sekiguchi (1986), initial formation conditions of clusters might also lead to a segregated distribution. Nevertheless, recent developments, both analytical and observational, indicate that mass segregation might be a natural consequence of the formation of the cluster and not just due to relaxation (Larson 2003). Simulations also confirm that competitive accretion naturally results in a mass-segregated cluster on the formation time-scale and does not require subsequent two-body relaxation (Bonnell et al. 2001).

We may conclude from the above discussion that the observed spatial mass segregation for this young cluster NGC 6530 might have resulted from a combination of initial conditions in the early stages of evolution and a subsequent relaxation process.

6 SUMMARY

The main points of the present work can be summarized as follows:

- (1) From the photographic plate data of Shanghai Astronomical Observatory with a time baseline of 87 years, the proper motions of 364 stars in the open cluster NGC 6530 region are reduced by a central overlapping technique, and the distribution parameters of the cluster and membership probabilities of individual stars in the cluster region are determined by the maximum likelihood principle, from which 250 member stars with membership probabilities higher than 0.9 are found.
- (2) It is demonstrated that the membership determination we made is successful and reliable, from which one can obtain an independent cluster member sample with more cluster members covering a larger observed area, which can be used for further studies of the cluster.
- (3) The CMD of NGC 6530 is obtained from our member sample, in which the effect of contamination of field stars is not serious. The CMD shows a well-defined blue envelope. This observational fact is very likely due to the presence of the giant molecular cloud, which prevents us from seeing the field stars behind.
- (4) Detailed analyses tell us that spatial mass segregation is present in NGC 6530, but there is no definite evidence for a velocity-mass (or velocity-luminosity) dependence, or a velocity mass segregation. The observed spatial mass segregation might be due to a combined effect of initial conditions and relaxation process.

Acknowledgements We would like to thank the staff in DAO, for their kind assistance in measuring the plates. Especially, L.C. wants to thank Dr. Peter Stetson for his kind help during his very pleasant stay at the DAO. This work is supported under the National Natural Science Foundation of China (Grant Nos. 10333020, 10333050 and 10373020) and the Shanghai Science Foundation (Grant No. 04ZR14153).

References

- van Altena W. F., Jones B. F. 1972, *A&A*, 20, 425 (AJ)
van den Bergh S., Sher D., 1960, *Pub. David, Dunlap. Obs.*, 2, 203
Balaguer-Núñez, L., Tian K. P., Zhao J. L., 1998, *A&AS*, 133, 387
Bonnell I. A., Bate M. R., Clarke C. J. et al., 2001, *MNRAS*, 323, 785
Cabrera-Cano J., Alfaro E. J., 1985, *A&A*, 150, 298
Chini R., Neckel Th., 1981, *A&A*, 102, 171
Damiani F., Flaccomio G., Micela G. et al., 2004, *ApJ*, 608, 781
Dias W. S., Alessi B. S., Moitinho A. et al., 2002, *A&A*, 389, 871
Eichhorn H. K., Williams C. A., 1963, *AJ*, 68, 221
Girard T. M., Grundy W. M., Lopez C. E. et al., 1989, *AJ*, 227, 98
Harris W. E., <http://physun.mcmaster.ca/harris/mwgc.dat>, 1999
Hiltner W. A., Morgan W. W., Neff J. S., 1965, *ApJ*, 141, 183
Jones B. F., Walker M. F., 1988, *AJ*, 95, 1755
Kerr F. J., Lynden-Bell D., 1986, *MNRAS*, 221, 1023
Kilambi G. C., 1977, *MNRAS*, 178, 423
Kumar B., Sagar R., Sanwal B. B. et al., 2004, *MNRAS*, 353, 991
Larson R. B., 1982, *Symposium on the Orion Nebula to Honor Henry Draper (Ann. N Y Acad. Sci.)*, 395, 274
Larson R. B., 2003, *ASP Conference Series*, 287, 65
Loktin A., Zakharonov P., Gerasimenko T. et al., 1997, *Baltic Astronomy*, 6, 316
Loktin A. V., Beshenov G. V., 2001, *Astro Lett.*, 27, 386
McCall M. L., Richer M. G., Visvanathan N., 1990, *ApJ*, 357, 502
McNamara B. J., Sekiguchi K., 1986, *AJ*, 310, 613
Prisinzano L., Damiani F., Micela G. et al., 2005, *A&A*, 430, 941
Ratnatunga K. U., Bahcall J. N., Casertano S., 1989, *ApJ*, 339, 106
Rauw G., Naze Y., Gosset E. et al., 2002, *A&A*, 395, 499
Russell J. L., 1976, Ph.D. thesis, University of Pittsburgh
Sagar R., Joshi U. C., 1978, *MNRAS*, 184, 467
Sanders W. L., 1971, *A&A*, 14, 226
Sung H., Chun M., Bessell M. S., 2000, *AJ*, 120, 333
The P. S., 1960, *ApJ*, 132, 40
Walker M. F., 1957, *ApJ*, 125, 636
Walker M. F., 1961, *ApJ*, 133, 1081
Wang J. J., Chen L., Zhao J. H., 1996, *Acta Astron. Sin.*, 37, 68
Vasilevskis S., Klemmola A., Preston G., 1958, *AJ*, 63, 387
Zhao J. L., He Y. P., 1987, *Acta Astron. Sin.*, 28, 374
Zhao J. L., He Y. P., 1990, *A&A*, 237, 54
Zhao J. L., Tian K. P., Su C. G., 1996, *Astrophysics and Space Science*, 235, 93